

# Shear Viscosity and Oscillations of Neutron Star Crust

A. I. Chugunov and D. G. Yakovlev

*Ioffe Physicotechnical Institute, St. Petersburg, Russia*

Received November 30, 2004; in final form, February 17, 2005

**Abstract**—We calculate the electron shear viscosity of dense matter (determined by Coulomb electron collisions) in a wide range of parameters typical for white dwarf cores and neutron star crusts. In the density range from  $\sim 10^3$  g/cm<sup>3</sup> to  $10^7$ – $10^{10}$  g/cm<sup>3</sup> we consider the matter composed of widely abundant astrophysical elements, from H to Fe. For higher densities,  $10^{10}$ – $10^{14}$  g/cm<sup>3</sup>, we employ the ground-state nuclear composition, taking into account finite sizes of atomic nuclei and the distribution of proton charge over the nucleus. Numerical values of the viscosity are approximated by an analytic expression convenient for applications. Using the approximation of plane-parallel layer, we study frequencies, eigenmodes, and viscous damping times of oscillations of high multipolarity,  $l \sim 500$ – $1000$ , localized in the outer crust of a neutron star. For instance, at  $l \sim 500$  oscillations have frequencies  $f \gtrsim 40$  kHz and are localized not deeper than about 300 m from the surface. When the crust temperature decreases from  $10^9$  K to  $10^7$  K, the dissipation time of these oscillations (with a few radial nodes) decreases from  $\sim 1$  year to 10–15 days.

© 2005 Pleiades Publishing, Inc.

## 1. INTRODUCTION

The shear viscosity of dense stellar material (with densities  $\rho \lesssim 10^{14}$  g/cm<sup>3</sup>) is important for a number of astrophysical problems, including the computations of the viscous damping of oscillations of white dwarves and the envelopes of neutron stars. The total shear viscosity can be presented as a sum of various matter components. In the case of the outer crust of a neutron star or the core of a white dwarf, it is determined by electrons and ions:  $\eta = \eta_e + \eta_i$ ; it is necessary to add a contribution due to free neutrons,  $\eta_n$ , in the inner crust of a neutron star. The electrons are strongly degenerate and form an ideal Fermi gas, while the ions are fully or partially ionized and form strongly nonideal Coulomb fluid or Coulomb crystal. Under these conditions, the electrons become the most important carriers of heat, charge (see, for example, [1]), and momentum, and the main process determining kinetic coefficients (thermal conductivity, electrical conductivity, and viscosity) is the scattering of electrons by ions (atomic nuclei).

The shear viscosity of the dense stellar material determined by electron–ion scattering has been considered in a number of papers. For example, the electron viscosity of a strongly nonideal Coulomb fluid was calculated in [2–4] from variational principle. The results of these computations are in good agreement. However, they were carried out without including the quasi-order of ions, which is important near the melting point. Inclusion of this quasi-order in a fluid together with multiple-phonon process of electron scattering in a crystal led to the disappearance of

appreciable (by a factor of two to four) jumps in the electrical and thermal conductivities [1].

Previous computations of the viscosity were carried out in the Born approximation. However, the non-Born corrections are important when calculating the electrical and thermal conductivities of matter containing chemical elements with high charge numbers  $Z$  (see, for example, [1]). We include these corrections and show that they are equally important for calculations of the viscosity.

When studying oscillations of the envelopes of neutron stars, it is necessary to know the viscosity of matter with the density of  $\rho \lesssim 10^{14}$  g/cm<sup>3</sup>. When  $\rho \sim 10^{13}$  g/cm<sup>3</sup>, the dimensions of atomic nuclei become comparable to the distances between them, and it is necessary to take into account the distribution of proton charge within the nuclei. This effect was included in the electrical- and thermal-conductivity computations of [5, 6] by introducing the form factor for the atomic nuclei. No such computations have been carried out for the viscosity.

In the current study, we have performed computations of the shear viscosity taking into account non-Born corrections and the form factor of the nuclei, the quasi-order in a Coulomb fluid, and multiphonon process in a Coulomb crystal. The results are approximated by analytical formulas that are convenient for astrophysical applications.

Various types of oscillation modes can be excited in neutron stars. Generally speaking, these oscillations carry important information about the internal

structure of neutron stars. Specific types of oscillations (such as r modes) can be accompanied by the radiation of gravitational waves. Interest in studies of neutron-star oscillations has been continuously growing. Since neutron stars are relativistic objects, theoretical studies of their oscillations must be carried out in the framework of general relativity. The relativistic theory of oscillations was developed in a series of papers by Thorne and coauthors [7–12]. In particular, the rapid ( $\sim 1$  s) damping of p-mode oscillations with multipolarity  $l = 2$  due to gravitational-wave radiation was demonstrated in [9]. Exact inclusion of general-relativistic effects is labor-intensive, but, in many cases, it is possible to use the relativistic Cowling approximation [13]. A similar analysis of various oscillation modes and mechanisms for their dissipation is carried out in [14]. We also note the recent review of Stergioulas [15], which contains an extensive bibliography. As a rule, oscillations with low values of  $l$  have been considered in the literature.

Although neutron stars are in the final stage of stellar evolution, they can be seismically active for many reasons. Possible mechanisms for the generation of oscillations have been widely discussed in the astrophysical literature (see, for example, [14, 15] and references therein). Much attention has recently been paid to r modes—vortex oscillations that can be generated in rapidly rotating neutron stars and are accompanied by powerful gravitational radiation. In addition, oscillations can be excited in neutron stars, for example, during X-ray bursts (nuclear explosions on the surfaces of accreting neutron stars), the bursting activity of magnetars (anomalous X-ray pulsars and soft gamma-ray repeaters; see, for example, [16]), and glitches (sudden changes of spin periods) of ordinary pulsars.

In this paper, we study the damping of oscillations in the context of illustrating the results of viscosity computations. We therefore choose the simplest example—p-mode oscillations that are localized in the outer crust due to a high value of the orbital number  $l \gtrsim 500$ .

## 2. SHEAR VISCOSITY OF DENSE STELLAR MATERIAL

### 2.1. Parameters of Equilibrium Dense Material

The state of strongly degenerate electrons can conveniently be described using their Fermi momentum  $p_F$  or wave number  $k_F$ :

$$p_F \equiv \hbar k_F = \hbar (3\pi^2 n_e)^{1/3} = m_e c x_r,$$

where  $\hbar$  is Planck's constant,  $m_e$  and  $n_e$  are the mass and number density of electrons,  $x_r \approx 1.009 (\rho_6 Z/A)^{1/3}$  is the relativistic parameter of the

electrons,  $Ze$  and  $A$  are the charge and atomic number of the ions (nuclei), and  $\rho_6$  is the density in units of  $10^6$  g/cm<sup>3</sup>. The electron degenerating temperature is

$$T_F = (\epsilon_F - m_e c^2) / k_B \\ \approx 5.93 \times 10^9 \left( \sqrt{1 + x_r^2} - 1 \right) \text{ K},$$

where  $k_B$  is Boltzmann's constant and

$$\epsilon_F \equiv m_e^* c^2 = m_e c^2 \sqrt{1 + x_r^2}$$

is the Fermi energy of electrons. In our study, we consider matter with  $T \ll T_F$  and  $T \lesssim 5 \times 10^9$  K (the latter is required in order to avoid dissociation of the atomic nuclei).

Further, we will use the Fermi velocity of the electrons:

$$v_F \equiv c \beta_r = p_F / m_e^*.$$

The electrostatic screening of a test charge by the degenerate electrons is described by the Thomas-Fermi wave number  $k_{TF}$  (the inverse screening radius):

$$k_{TF}^2 = 4\pi e^2 \frac{\partial n_e}{\partial \mu} \approx \frac{\alpha}{\pi \beta_r} (2k_F)^2,$$

where  $\mu \approx \epsilon_F$  is the chemical potential of electrons and  $\alpha = e^2 / \hbar c \approx 1/137.036$  is the fine-structure constant.

The state of the system of ions is described by the classical Coulomb coupling parameter

$$\Gamma = \frac{Z^2 e^2}{a k_B T} \approx \frac{22.75 Z^2}{T_6} \left( \frac{\rho_6}{A} \right)^{1/3},$$

where  $a = (3/4\pi n_i)^{1/3}$  is the radius of the ion sphere;  $n_i = n_e/Z$ , the number density of ions; and  $T_6$ , the temperature in units of  $10^6$  K. When  $\Gamma \ll 1$ , the ions form a nearly ideal Boltzmann gas. If  $\Gamma \gtrsim 1$ , they form a strongly nonideal Coulomb fluid. Finally, when  $\Gamma > \Gamma_m$  (corresponding to temperatures  $T < T_m$ ), the ions crystallize. The crystallization of a classical system of ions corresponds to  $\Gamma_m \approx 175$  (see, for example, [17]).

Quantum effects in the system of ions become important when  $\Theta \equiv T/T_p \ll 1$ , where

$$T_p = \hbar \omega_p / k_B \approx 7.832 \times 10^6 (Z/A) \rho_6^{1/2} \text{ K}$$

is the ion plasma temperature,  $\omega_p = (4\pi Z^2 e^2 n_i / m_i)^{1/2}$  is the ion plasma frequency,  $m_i = Am_u$  is the mass of an ion, and  $m_u = 1.6605 \times 10^{-24}$  g is the atomic mass unit.

## 2.2. General Formalism

In the case of isotropic matter, the viscous-stress tensor has the simple form

$$\sigma'_{\alpha\beta} = \eta \left( \frac{\partial U_\alpha}{\partial x_\beta} + \frac{\partial U_\beta}{\partial x_\alpha} - \frac{2}{3} \delta_{\alpha\beta} \nabla \cdot \mathbf{U} \right) + \zeta \delta_{\alpha\beta} \nabla \cdot \mathbf{U}, \quad (1)$$

where  $\mathbf{U}$  is the hydrodynamical velocity of the matter,  $\eta$  is the shear viscosity, and  $\zeta$  is the bulk viscosity (this last quantity is especially important for the uniform compression and rarefaction of matter).

Generally speaking, crystalline matter is anisotropic, and expression (1) for the viscous-stress tensor may not be formally applicable. However, in dense matter, ions crystallize with the formation of a high-symmetry face or body centered cubic lattice. In this case, the viscous-stress tensor for a monocrystal is determined by three independent coefficients (see, for example, [18]), and can be written in the form (1) with an additional term of the form  $\kappa \delta_{\alpha\beta} \partial U_\alpha / \partial x_\alpha$  (the sum over  $\alpha$  is not carried out). The quantity  $\mathbf{U}$  should be understood as the velocity field for shifts of the ions in their lattice sites. When studying any transport processes on scales exceeding the characteristic monocrystal size, the matter can be considered to be isotropic. As in all the literature concerned with the kinetics of the crystalline matter of white dwarves and neutron stars without magnetic fields, we will restrict our analysis to this case (assuming  $\kappa = 0$ ).

The shear viscosity of the envelopes of neutron stars and the cores of white dwarves is primarily determined by the strongly degenerate electrons. It is convenient to present this viscosity in the form

$$\eta_e = \frac{n_e p_F v_F}{5\nu_e},$$

where  $\nu_e = 1/\tau_e$  is the effective electron collision frequency, which is related to the effective electrons relaxation time  $\tau_e$ . If the electron scattering is determined by several independent processes, these can be studied separately, and the total collision frequency will be the sum of the partial ones. For the dense matter of white dwarf cores and envelopes of neutron stars,

$$\nu_e = \nu_{ei} + \nu_{imp} + \nu_{ee},$$

where  $\nu_{ei}$ ,  $\nu_{imp}$ , and  $\nu_{ee}$  correspond to electron scattering by ions, impurity atoms, and electrons, respectively. The dominant process is electron–ion scattering, to which the current paper is dedicated. Electron–ion scattering also determines the thermal and electrical conductivities of dense matter (see, for example, [1]). With small variations, the formalism proposed by Potekhin *et al.* [1] is also applicable for computations of the viscosity.

In crystalline matter, the electron–ion interaction can adequately be described in terms of the emission and absorption of phonons [19]. This description can be realized using an ion dynamical structure factor [2].

The frequency of electron–ion collisions (*ei* scatterings) can be written as

$$\nu_{ei} = 12\pi \frac{Z^2 e^2 \Lambda_{ei} n_i}{p_F^2 v_F} = \frac{4Z\epsilon_F}{\pi\hbar} \alpha^2 \Lambda_{ei}, \quad (2)$$

where  $\Lambda_{ei}$  is the effective Coulomb logarithm, which can be calculated using the variational method (see, for example, [19]). When using the simplest trial function in the Born approximation for a strongly nonideal ion plasma ( $\Gamma \gtrsim 1$ ), one obtains

$$\Lambda_{ei} = \int_{q_0}^{2k_F} q^3 u^2(q) \left( 1 - \frac{q^2}{4k_F^2} \right) \times \left[ 1 - \frac{1}{4} \left( \frac{\hbar q}{m_e^* c} \right)^2 \right] S_\eta(q) dq, \quad (3)$$

where  $q_0$  is the minimum momentum transferred in an *ei* scattering event;  $q_0 = 0$  for the liquid phase and  $q_0 = q_B$  in the crystalline phase, where  $q_B = (6\pi n_i)^{1/3}$  is the radius of a sphere of the same volume as the Brillouin zone. The value  $q_0 = q_B$  was intended to select umklapp processes (i.e., those involving variations in the electron momentum  $\gtrsim \hbar q_B$ ) in an *ei* scattering event. At temperatures that are not too low, the contribution of such processes to the Coulomb logarithm  $\Lambda_{ei}$ ,

$$T \gtrsim T_u \sim T_p Z^{1/3} \alpha / 3\beta_r,$$

is much higher than the contribution of normal processes occurring when  $q < q_B$  (see, for example, [20]). However, at low temperatures ( $T \lesssim T_u$ ), umklapp processes are “frozen” and the viscosity is determined by normal processes. We will neglect this effect below, restricting our consideration to temperatures  $T \gtrsim T_u$ .

The function  $u(q)$  in (3) describes the Coulomb interaction between an electron and an atomic nucleus, as discussed in Section 2.3. The factor in square brackets describes the kinematic effect of the backward scattering of the relativistic electrons (see, for example, [21]);  $S_\eta(q)$  is an effective static structure factor that takes into account ion correlations. This factor coincides with the effective structure factor determining the electrical resistivity of the dense matter, which was computed and approximated in [22]. Note that the structure factor of a strongly nonideal Coulomb fluid is known only in the classical limit ( $\Theta \gg 1$ ). We also define a *simplified* structure factor, based on the following approximations:

- Neglecting quasi-ordering in ion positions in the Coulomb fluid (see, for example, [1]).

- Single-phonon approximation for the inelastic structure factor of the Coulomb crystal (see, for example, [20]).

We will call the viscosity calculated using the simplified structure factor the *simplified* viscosity. Note that previous computations of the shear viscosity by Flower and Itoh [2, 3] and Nandkumar and Pethick [4] were carried out for a Coulomb fluid using the simplified structure factor.

To take into account corrections to the Born approximation, we also multiply the integrand by the ratio of the exact and Born cross sections for Coulomb scattering. This method was proposed in [23] and was used to calculate the transport coefficients by Potekhin *et al.* [1, 24].

The effective frequency of electron scattering by impurities (assuming that the impurity atoms randomly occupy some of the sites of the crystal lattice) is similar to the frequency of scattering by ions [see (2)]:

$$\nu_{\text{imp}} = \frac{12\pi e^4}{p_F^2 v_F} \sum_{\text{imp}} (Z - Z_{\text{imp}})^2 n_{\text{imp}} \Lambda_{\text{imp}},$$

where  $Z_{\text{imp}}$  is the charge number of the impurity ion and the Coulomb logarithm  $\Lambda_{\text{imp}}$  is calculated using (3), but assuming the impurity atoms are only weakly correlated (corresponding to the structure factor  $S_{\text{imp}} \equiv 1$ , while the screening of the impurities is taken into account in the factor  $u(q)$ ). In the simplest model with Debye screening (with a screening radius of  $q_{S_{\text{imp}}}^{-1}$ ),

$$\Lambda_{\text{imp}} = \frac{1}{2} (1 + 3\beta_r^2 \xi^2 + 2\xi + 2\xi\beta_r^2) \times \ln \left( \frac{1 + \xi}{\xi} \right) - \frac{3}{2}\beta_r^2 \xi - \frac{1}{4}\beta_r^2 - 1,$$

where  $\xi = q_{S_{\text{imp}}}/(2k_F)$  and  $q_{S_{\text{imp}}}^2 = k_{\text{TF}}^2 + k_{\text{imp}}^2$ . Here,  $k_{\text{imp}}$  is the wave number for the Debye screening of the test charge by impurities (the inverse correlation length of the impurities). This weakly influences the result ( $k_{\text{TF}} \gg k_{\text{imp}}$ ), and can be estimated as  $k_{\text{imp}} = (4\pi n_{\text{imp}}/3)^{1/3}$ , where  $n_{\text{imp}}$  is the number density of the impurities. Scattering on impurities is important at low temperatures, when scattering on the crystal lattice is suppressed by quantum effects.

The expression for the frequency of electron-electron collisions  $\nu_{ee}$  was obtained by Flowers and Itoh [2]. Their result can be written in the form

$$\nu_{ee} = \frac{5\pi^2 \alpha^2 k_B^2 T^2}{2m_e^* c^2 \hbar} \left( \frac{k_F}{k_{\text{TF}}} \right) \left( 1 + \frac{6}{5x_r^2} + \frac{2}{5x_r^4} \right) \quad (4)$$

$$\approx 4.473 \times 10^{11} \left( \frac{k_F}{k_{\text{TF}}} \right) \left( \frac{n_0}{n_e} \right)^{1/3} T_8^2 \text{ s}^{-1},$$

where the latter expression is presented for an ultra-relativistic electron gas ( $x_r \gg 1$ ),  $n_0 \approx 0.16 \text{ fermi}^{-3}$  is the number density of nucleons in the atomic nuclei, and  $T_8$  is the temperature in units of  $10^8 \text{ K}$ .

### 2.3. The Form Factor of the Atomic Nuclei

The function  $u(q)$  describing the Coulomb interaction between an electron and an ion in (3) has the form

$$u(q) = \frac{F(q)}{q^2 |\varepsilon(q)|},$$

where  $\varepsilon(q)$  is the static longitudinal dielectric function of the degenerate electron gas [25], which describes the electronic screening of the ion field. Here,

$$F(q) \equiv \frac{1}{Z} \int e n_p(\mathbf{r}) \exp(i\mathbf{r} \cdot \mathbf{q}) dV \quad (5)$$

$$= \frac{4\pi e}{Z} \int_0^{r_p} \frac{n_p(r) \sin(qr)}{q} r dr$$

is the nuclear form factor characterizing the distribution of proton charge within the atomic nucleus. The integration in (5) is carried out over the atomic nucleus,  $n_p(\mathbf{r})$  is the local number density of protons, and  $r_p$  is the radius of the proton core. In white dwarves and the outer envelopes of neutrons stars ( $\rho \lesssim 10^{11} \text{ g/cm}^3$ ), the atomic nuclei can be taken to be pointlike,  $F(q) \equiv 1$ . At densities  $\rho \lesssim 10^{13} \text{ g/cm}^3$ , the proton charge can with good accuracy be taken to be uniformly distributed throughout the nucleus. In this case, it is a good approximation to write the form factor as

$$F(q) = \frac{3}{(qr_p)^3} [\sin(qr_p) - qr_p \cos(qr_p)], \quad (6)$$

where  $r_p$  is the radius of the proton core in the atomic nucleus. When  $\rho \gtrsim 10^{13} \text{ g/cm}^3$ , the proton-density profile differs strongly from a step function, and the form factor (6) becomes unacceptable. In this case, we determined the nuclear form factor using the model of the ground-state matter with smoothed dependences of the parameters on the density of the matter [26].

### 2.4. Analytical Approximation for the Viscosity

We have obtained an analytical approximation for the Coulomb logarithm of *ei* scattering using the method of the *effective electron-ion scattering potential* proposed in [1] for the electrical and thermal conductivities. The properties of matter with the density of  $\rho \lesssim 10^{10} \text{ g/cm}^3$  were studied in [1], where

the form factor of the atomic nuclei was taken to be unity. Later, Gnedin *et al.* [27] extended this method to higher densities. As we noted above, the effective structure factors for the viscosity and electrical conductivity coincide. This simplifies generalization of the effective-potential method for the approximation of the shear viscosity. Following [27], we write in place of  $u^2(q)S_\eta(q)$  in (3)

$$\begin{aligned} [u^2(q)S_\eta(q)]_{\text{eff}} &= \frac{1}{(q^2 + q_S^2)^2} \\ &\times \left[ 1 - e^{-s_0 q^2} \right] e^{-s_1 q^2} G_\eta D. \end{aligned} \quad (7)$$

The factor  $(q^2 + q_S^2)^{-2}$  corresponds to Debye screening of the Coulomb interaction with the effective screening radius  $q_S^{-1}$ ; the term in square brackets describes the ion correlations. The functions  $G_\eta$  and  $D$  describe ion quantum effects. The factor  $\exp(-s_1 q^2)$  added in [27] takes into account the influence of the atomic-nucleus form factor. The numerical values of the shear viscosity obtained based on the exact theory are reproduced for the same parameters as the electrical and thermal conductivities in [27]:

$$\begin{aligned} s &\equiv \left( \frac{q_S}{2k_F} \right)^2 = (s_i + s_e) e^{-\beta Z}; \\ \beta Z &= \pi \alpha Z \beta_r; \quad s_i = s_D (1 + 0.06\Gamma) e^{-\sqrt{\Gamma}}; \\ s_D &= (2k_F r_D)^{-2}; \\ w &\equiv (2k_F)^2 s_0 = \frac{u_{-2}}{s_D} \left( 1 + \frac{\beta Z}{3} \right); \\ w_1 &\equiv (2k_F)^2 s_1 = 14.73 x_{\text{nuc}}^2 \\ &\times \left( 1 + \frac{Z}{13} \sqrt{x_{\text{nuc}}} \right) \left( 1 + \frac{\beta Z}{3} \right); \\ G_\eta &= (1 + 0.122\beta_Z^2) \left( 1 + 0.0361 \frac{Z^{-1/3}}{\Theta^2} \right)^{-1/2}; \\ D &= \exp \left[ -0.42 u_{-1} \sqrt{\frac{x_r}{AZ}} \exp(-9.1\Theta) \right], \end{aligned}$$

where  $s_e \equiv k_{\text{TF}}^2 / (2k_F)^2 = \alpha / \pi \beta_r$  is the electron-screening parameter,  $r_D = a / \sqrt{3\Gamma}$  is the ionic Debye radius,  $x_{\text{nuc}}$  is the ratio of the mean-square radius of the distribution of the protons in the atomic nucleus and the radius of the ion sphere, and  $u_{-1} \approx 2.8$  and  $u_{-2} \approx 13$  are the parameters of the phonon spectrum in the Coulomb crystal. Note that the function  $G_\eta$  coincides with the function  $G_\sigma$  from [27].

After integrating in (3) with the effective potential (7), we obtain

$$\Lambda = [\Lambda_0(s, w + w_1) - \Lambda_0(s, w_1)] G_\eta D,$$

where the functions

$$\begin{aligned} \Lambda_0(s, w) &= \Lambda_1(s, w) \\ &- (1 + \beta_r^2) \Lambda_2(s, w) + \beta_r^2 \Lambda_3(s, w), \end{aligned}$$

with

$$\begin{aligned} 2\Lambda_1(s, w) &= \ln \frac{s+1}{s} + \frac{s}{s+1} (1 - e^{-w}) \\ &- (1 + sw) e^{sw} [E_1(sw) - E_1(sw+w)], \\ 2\Lambda_2(s, w) &= \frac{e^{-w} - 1 + w}{w} \\ &- \frac{s^2}{s+1} (1 - e^{-w}) - 2s \ln \frac{s+1}{s} \\ &+ s(2 + sw) e^{sw} [E_1(sw) - E_1(sw+w)], \\ 2\Lambda_3(s, w) &= 3s^2 \ln \frac{1+s}{s} + \frac{1}{2} \frac{2s^3 - 4s^2 - 3s + 1}{1+s} \\ &- \frac{s^3}{(1+s)} e^{-w} + \frac{e^{-w}}{w} + \frac{(2sw-1)(1-e^{-w})}{w^2} \\ &- s^2(3 + sw) e^{sw} (E_1(sw) - E_1(sw+w)). \end{aligned}$$

Here,  $E_1(x) \equiv \int_x^\infty y^{-1} e^{-y} dy$  is the exponential integral (see, for example, [28]). The maximum error in the approximation for the viscosity does not exceed 20%.

## 2.5. Main Properties of the Shear Viscosity

Let us discuss the results of our computations of the shear viscosity without taking into account the freezing out of umklapp processes (Section 2.2). Figure 1 presents the temperature dependence of the shear viscosity for a carbon plasma with density  $\rho = 10^4 \text{ g/cm}^3$ . The upper horizontal scale plots the non-ideality parameter  $\Gamma$  of the plasma. Since the charge number is fairly low,  $Z = 6$ , the non-Born corrections are modest, and are not visible on the scale of Fig. 1. All the data presented in the figure except for the dot-dashed curves correspond to the scattering of electrons by ions of single type.

The bold points in the figure show the numerical results. The solid curve is the analytical approximation for the viscosity. The dashed curve shows the viscosity computed using the simplified structure factor (Section 2.2). The large jumps in this ‘‘simplified’’ viscosity at the melting point are clearly visible. These jumps (by a factor of two to four) are present for all chemical elements and all plasma parameters. Modification of the structure factor (Section 2.2) increases the accuracy of the computations in the liquid and solid phases, and makes the viscosity jumps insignificant for all elements. This makes it possible to introduce a single approximation for both phases (Section 2.4).

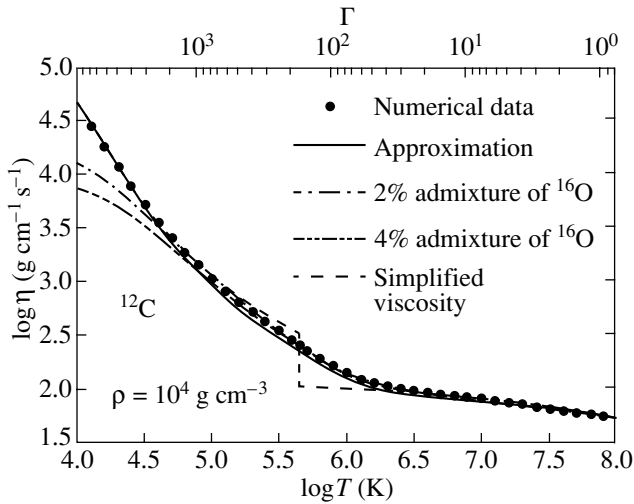


**Fig. 1.** Temperature dependence of the shear viscosity for a carbon plasma with density  $\rho = 10^4 \text{ g/cm}^3$ . The solid curve shows the analytical approximation of the viscosity. The bold points present the results of the numerical calculations. The dashed curve shows the “simplified” viscosity, which demonstrates a jump at the melting point. The dot-dashed curves correspond to matter with  $^{16}\text{O}$  impurities with concentration of 2 and 4%.

However, appreciable viscosity jumps are present at the melting point in our computations for high densities, where zero point oscillations of ions become important. We assume, as did Potekhin *et al.* [1] for the electrical and thermal conductivity, that these jumps are a consequence of using the classical structure factor in the ion fluid under conditions when quantum effects are important (while quantum effects are included in the solid phase). Since the numerical data used to construct the analytical approximation include both the liquid and solid phases, the general analytical approximation shifts the viscosity in the liquid phase to the viscosity in the solid phase. We suppose that, for an ionic fluid at high densities, this approximation is more exact than our original numerical data. It will be possible to verify this in the future, when the ionic structure factors in a fluid are calculated taking into account quantum effects.

The dot-dashed curves in Fig. 1 demonstrate the influence of scattering by charged impurities. We considered oxygen impurities with concentrations of 2 and 4%. The presence of these impurities weakly manifested at high temperatures, but dominates at low temperatures,  $T \ll T_p$ , when scattering of electrons by phonons in the Coulomb crystal is strongly suppressed by quantum effects.

Figure 2 presents the temperature dependence of the shear viscosity for an iron plasma with density  $\rho = 10^8 \text{ g/cm}^3$ . The upper horizontal scale plots the plasma nonideality parameter  $\Gamma$ . The bold points

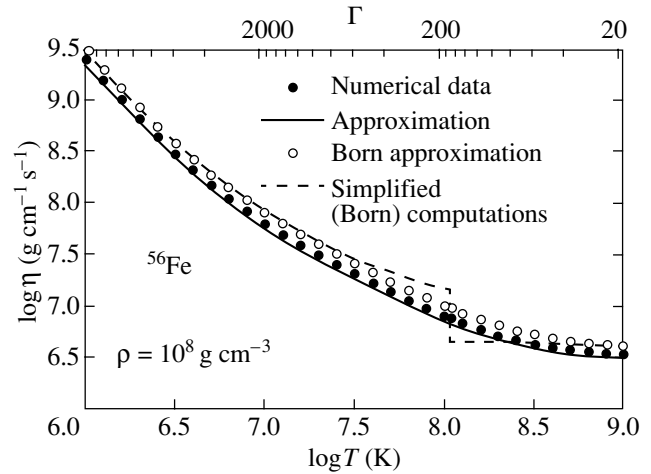


**Fig. 2.** Temperature dependence of the shear viscosity for an iron plasma with density  $\rho = 10^8 \text{ g/cm}^3$ . The solid curve shows the analytical approximation of the viscosity. The bold points present the results of the numerical computations. The hollow circles correspond to the Born approximation. The dashed curve presents the “simplified” viscosity computed in the Born approximation.

present our numerical results, while the solid curve shows the approximation. The dashed curve depicts the computations using the simplified structure factor neglecting non-Born corrections. As in Fig. 1, the simplified viscosity displays jumps at the melting point, while the new results pass smoothly through this point. The charge number of iron ( $Z = 26$ ) is high enough for the non-Born corrections to be appreciable. To demonstrate this effect, the hollow circles in Fig. 2 show the results of numerical computations of the viscosity in the Born approximation. We can see that the non-Born corrections reduce the viscosity by approximately 20%.

Figure 3 depicts the density dependence of the shear viscosity for hydrogen, helium, carbon, and iron plasmas at a temperature of  $T = 10^7 \text{ K}$ . Let us consider the densities typical for the cores of white dwarves and the outer envelopes of neutron stars. The bold points show the numerical results, and the curves are the approximations. The strong dependence of the plasma viscosity on the chemical composition is due to the dependence of the frequency of electron–ion collisions on the charge number  $Z$ . In contrast to the thermal conductivity (see, for example, [1]), the influence of electron–electron collisions on the viscosity is insignificant at the considered densities, even for hydrogen.

Figure 4 demonstrates the density dependence of the shear viscosity of the plasma in the range from  $10^6$  to  $10^{15} \text{ g/cm}^3$  for the three temperatures  $T = 10^7, 10^8, 10^9 \text{ K}$ . The ground state nuclear composition with smoothed parameters was used. The points

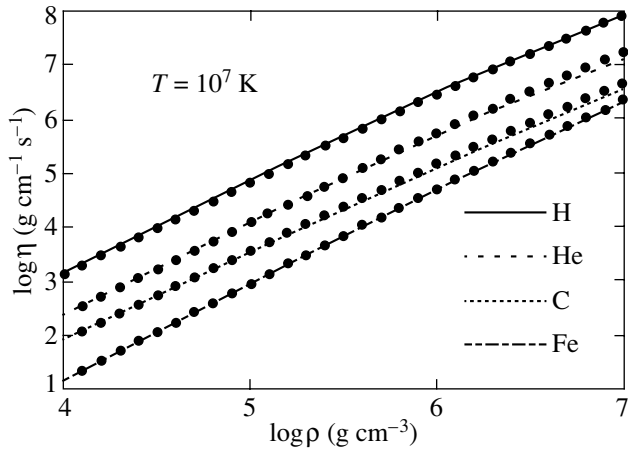


**Fig. 3.** Shear viscosity of a plasma at temperature  $T = 10^7$  K as a function of the density for various chemical compositions (H, He, C, and Fe). The bold points show the numerical results and the curves show the analytic fit.

show the numerical results, and the curves are the approximations. In contrast to the thermal conductivity [1], the shear viscosity decreases strongly with growing temperature. Note that the ratio  $\rho/\eta$  grows with increasing density in the outer crust of a neutron star. These results are important when computing the damping of oscillations in the crust of a neutron star (see Section 3.3).

For illustrative purposes, the plot is continued beyond the crust into the stellar core (densities  $\rho \geq 1.5 \times 10^{14}$  g/cm<sup>3</sup>). In the core, we used the equation of state of the matter presented in [29]. It is assumed that the core material consists of neutrons, protons, and electrons and is not superfluid. The electronic viscosity in the core of such a star is primarily determined by the scattering of electrons by the degenerate protons. The corresponding collision frequency is obtained analogously to the rate of electron-electron collisions [see (4)], and is equal to

$$\begin{aligned} \nu_{ep} &= \pi^2 \alpha^2 \left( \frac{k_F}{q_0} \right) \frac{(k_B T)^2 m_p^{*2}}{\hbar p_F^3} c \\ &\approx 1.434 \times 10^{12} \left( \frac{k_F}{q_0} \right) T_8^2 \left( \frac{m_p^*}{m_p} \right)^2 \frac{n_0}{n_e} \text{ s}^{-1}, \end{aligned}$$

where  $m_p \approx 1.672 \times 10^{-24}$  g is the proton mass and  $m_p^*$  is its effective mass, which differs from  $m_p$  due to multiple-frequency effects (it is assumed that  $m_p^* = 0.7m_p$ ). The Debye-screening parameter in the stellar core is equal to

$$q_0^2 = 4\pi \sum_j e_j^2 \frac{\partial n_j}{\partial \mu_j},$$

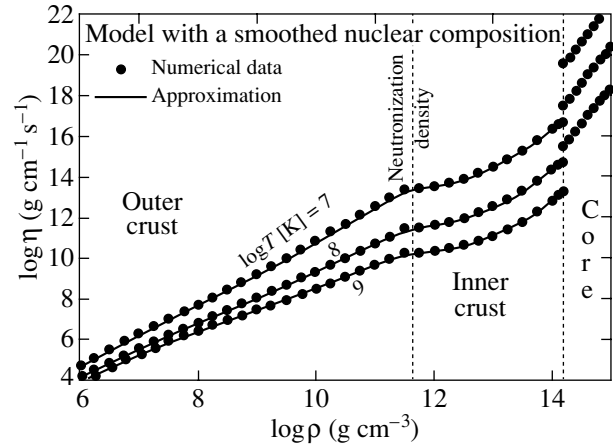


**Fig. 4.** Shear viscosity of the ground state matter as a function of the density  $\rho$  for the three temperatures  $T = 10^7, 10^8, 10^9$  K. The solid curves show the analytical approximation of the viscosity. The bold points represent the results of our numerical computations. The vertical dotted lines indicate the neutron drip density and the boundaries of the crust and core of a neutron star ( $\rho = 1.5 \times 10^{14}$  g/cm<sup>3</sup> in our computations). The electronic viscosity in the stellar core determined by the scattering of electrons by degenerate protons is presented for comparison.

where the sum is taken over all types of charged particles (electrons and protons);  $e_j$ ,  $n_j$ , and  $\mu_j$  are the charge, number density, and chemical potential of particles of sort  $j$ . Due to the strong suppression of scattering by the proton degeneracy, the electronic viscosity in the core grows by approximately a factor of 1000 compared to its value in the crust.

### 3. P MODES OF OSCILLATIONS OF A NEUTRON STAR CRUST

This section is dedicated to a study of the p modes of the oscillations (i.e., oscillations in which perturbations of the pressure dominate over the buoyant force) with high orbital numbers (multipolarity),  $l \gtrsim 500$ , localized in the outer crust of a nonrotating neutron star.

#### 3.1. General Formalism

##### 3.1.1. Flat Metric for the Envelope of a Nonrotating Neutron Star

The standard spacetime metric for a nonrotating neutron star [30] can be written as

$$ds^2 = c^2 e^{2\Phi} d\tilde{t}^2 - e^{2\lambda} dr^2 - r^2 d\Omega^2, \quad (8)$$

where  $d\Omega^2 = d\theta^2 + \sin^2 \theta d\varphi^2$ ,  $\tilde{t}$  is the time coordinate,  $r$  is the radial coordinate,  $\theta$  and  $\varphi$  are the polar and azimuthal angles, and the functions  $\lambda(r)$  and  $\Phi(r)$  determine the curvature of spacetime. In the

case of interest to us of the thin envelope, we can neglect variation of the functions  $\lambda(r)$  and  $\Phi(r)$  on the scale of the crust and use the value at the stellar surface:

$$e^{2\Phi(R)} = e^{-2\lambda(R)} = 1 - \frac{2GM}{c^2 R},$$

where  $M$  is the gravitational mass of the neutron star. Neglecting variations in  $r$  in the envelope compared to the stellar radius  $R$  (in the approximation of a thin envelope layer), we can rewrite (8) in the form

$$ds^2 = c^2 \left(1 - \frac{R_G}{R}\right) dt^2 - \left(1 - \frac{R_G}{R}\right)^{-1} dr^2 - R^2 d\Omega^2,$$

where  $R_G = 2GM/c^2 \approx 2.953(M/M_\odot)$  km is the gravitational radius. Introduction of the local time  $t$  and local depth  $z$ , specified by the relations

$$t = \tilde{t} \sqrt{1 - R_G/R}, \quad z = (R - r) / \sqrt{1 - R_G/R}, \quad (9)$$

we come to a flat coordinate system that is the same for the entire neutron-star crust:

$$ds^2 = c^2 dt^2 - dz^2 - R^2 d\Omega^2. \quad (10)$$

This metric coincides with the metric of a thin spherical layer in a flat spacetime.

### 3.1.2. Equilibrium Structure of the Neutron Star Crust

The structure of the neutron star is determined by the equation of hydrostatic equilibrium, including the effects of general relativity (the Tolman-Oppenheimer-Volkov equation; see, for example, [30]). This equation is greatly simplified in the envelope, and can be rewritten in the planar coordinate system (9):

$$c_s^2 \frac{d\rho_0}{dz} = \frac{dP_0}{dz} = g\rho_0, \quad (11)$$

where  $P_0$  and  $\rho_0$  are the equilibrium pressure and density,  $c_s^2 \equiv \partial P_0 / \partial \rho_0$  is the square of the local sound speed, and

$$g = \frac{GM}{R^2 \sqrt{1 - R_G/R}} \approx 1.327 \times 10^{14} \frac{M}{M_\odot} \left(\frac{10 \text{ km}}{R}\right)^2 / \sqrt{1 - R_G/R} \frac{\text{cm}}{\text{s}^2}$$

is the gravitational acceleration.

The computations used the equation of state for a fully degenerate electron gas with electrostatic correction to the pressure. The chemical composition

of the matter was determined using a model with a smoothed equilibrium nuclear composition. We also used a polytropic model for the envelope, in which the pressure is determined by the degenerate electrons, which are taken to be relativistic at all densities, and the matter is assumed to consist of  $^{56}\text{Fe}$  nuclei.

### 3.1.3. Oscillation Equation

In the outer envelopes of neutrons stars, the main contribution to the pressure is produced by the degenerate electrons. Therefore, when considering the p modes of the oscillations, we can use a single equation of state to describe the equilibrium configuration of the star and perturbations.

Let us write the Euler equation in a planar metric (10):

$$\frac{\partial \mathbf{U}}{\partial t} + (\mathbf{U} \cdot \nabla) \mathbf{U} = -\frac{\nabla P}{\rho} + \mathbf{g},$$

where  $P$  is the pressure of the matter. The continuity equation must also be satisfied:

$$\frac{\partial \rho}{\partial t} + \nabla(\rho \mathbf{U}) = 0.$$

Taking the velocity  $\mathbf{U}$  to be small and introducing Euler perturbations of the pressure  $\delta P = P - P_0$  and density  $\delta \rho = \rho - \rho_0$ , we obtain the linearized Euler equation

$$\frac{\partial \mathbf{U}}{\partial t} = \frac{\delta \rho}{\rho_0^2} \nabla P_0 - \frac{1}{\rho_0} \nabla \delta P$$

and the continuity equation

$$\frac{\partial \delta \rho}{\partial t} + \nabla(\rho_0 \mathbf{U}) = 0, \quad (12)$$

while the equation of state for the perturbations can be rewritten in the form

$$\delta P = c_s^2 \delta \rho. \quad (13)$$

We will consider irrotational motion and write the velocity in the form  $\mathbf{U} = \nabla \phi$ , where  $\phi$  is the velocity potential, which is a scalar function of coordinates and time. Formally, the function  $\phi$  is determined with accuracy to within an arbitrary function of time, which we choose so that the Euler equation can be rewritten [using (11) and (13)]

$$\frac{\partial \phi}{\partial t} = -\frac{\delta P}{\rho_0} = -c_s^2 \frac{\delta \rho}{\rho_0}. \quad (14)$$

Differentiating (14) with respect to the local time  $t$  and taking into account (12) and (11) yields

$$\frac{\partial^2 \phi}{\partial t^2} = c_s^2 \Delta \phi + \mathbf{g} \cdot \nabla \phi, \quad (15)$$

where we have introduced the Laplace operator

$$\Delta \approx \frac{\partial^2}{\partial z^2} + \frac{1}{R^2} \left( \frac{\partial^2}{\partial \theta^2} + \frac{1}{\sin^2 \theta} \frac{\partial^2}{\partial \varphi^2} \right).$$

An equation that coincides with (15) was obtained by Lamb [31] for atmospheric oscillations. The variables in (15) can be separated if we write

$$\phi = e^{i\omega t} Y_{lm}(\Omega) F(r),$$

where  $\omega$  is the oscillation frequency,  $Y_{lm}(\Omega)$  are spherical harmonic functions (see, for example, [32]), and  $F(z)$  is an unknown function of depth that is determined by the equation

$$\frac{d^2 F}{dz^2} + \frac{g}{c_s^2} \frac{dF}{dz} + \left( \frac{\omega^2}{c_s^2} - \frac{l(l+1)}{R^2} \right) F = 0. \quad (16)$$

The first boundary condition for this equation,

$$\text{function } F(z) \text{ is bounded as } z \rightarrow 0, \quad (17)$$

follows from the requirement that the amplitude of the oscillations at the stellar surface be finite. The second boundary condition is imposed artificially. In the current study, we solved equations that were applicable only in the thin crust of the star. Therefore, the oscillations should become damped with depth. For simplicity, we formally move this boundary condition to infinity along  $z$  and will monitor the true region of localization of the oscillations (see Section 3.3). In this case, the boundary condition can be written

$$F(z) \rightarrow 0 \text{ as } z \rightarrow \infty. \quad (18)$$

Together with the boundary conditions (17) and (18), Eq. (16) specifies the eigenfrequencies and modes of the oscillations. Moreover, the following asymptotics are valid at large and small depths:

$$F(z) \propto \begin{cases} 1 - \omega^2 z/g & z \rightarrow 0, \\ \exp\left(-\sqrt{l(l+1)}z/R\right) & z \rightarrow \infty. \end{cases} \quad (19)$$

Perturbations of the pressure and density are expressed in terms of the function  $\phi(\mathbf{r})$  using relation (14):

$$\delta P = -i\omega\rho_0\phi, \quad \delta\rho = \frac{\delta P}{c_s^2} = -i\frac{\omega\rho_0}{c_s^2}\phi.$$

Due to the boundary condition (17), variations of the pressure and density,  $\delta P$  and  $\delta\rho$ , are zero at the stellar surface (since  $\rho_0(R) = 0$ ). We can see from these last expressions that the number of zeros of the velocity potential with depth ( $k$ ) coincides with the number of nodes of the pressure and density variations. Further, we will call  $k$  the *number of radial nodes of the mode*.

The displacement vector for a matter element in the case of oscillations can be written in the form

$$\boldsymbol{\xi} \equiv \int \mathbf{U} dt = -\frac{i}{\omega} \nabla \cdot \phi.$$

The  $z$  component of this vector is

$$\xi_z = -\frac{i}{\omega} Y_{lm}(\theta, \varphi) \frac{dF}{dz},$$

and the magnitude of the horizontal displacement can be estimated as

$$|\xi_h| \approx \frac{l}{\omega R} |F(z)|.$$

The quantities  $lF(z)/R$  and  $dF/dz$  appear on equal footing in (16). Therefore, horizontal and radial displacements should have the same order of magnitude for the oscillations considered.

Oscillations of a polytropic envelope in a plane-parallel approximation were studied earlier by Goch [33] assuming that the equation of state of the unperturbed matter and the perturbations are described by polytropes with different indices. In the limiting case of equal polytropic indices  $n$ , his result can be presented as follows: the mode containing  $k$  radial nodes has the eigenfrequency

$$\omega_k^2 = \frac{g}{R} \sqrt{l(l+1)} \left( \frac{2k}{n} + 1 \right) \quad (20)$$

$$\approx 10^8 g_{14} \left( \frac{10 \text{ km}}{R} \right) \sqrt{l(l+1)} \left( \frac{2k}{n} + 1 \right) \text{ s}^{-2},$$

while the velocity potential is specified by the function

$$F_k(z) = \exp\left(-\sqrt{l(l+1)}\frac{z}{R}\right) \times L_k^{(n-1)}\left(2\sqrt{l(l+1)}\frac{z}{R}\right),$$

where  $L_k^{(n-1)}(x)$  is a generalized Laguerre polynomial (see, for example, [28]) and  $g_{14}$  is the gravitational acceleration at the stellar surface in units of  $10^{14} \text{ cm/s}^2$ . Note that the eigenfrequencies agree with the simple estimate  $\omega^2 \sim g/a$ , where  $a \sim R/l$  is the characteristic scale for the localization of the oscillations.

Note that the mode with  $k = 0$  does not have any radial nodes. It corresponds to the vanishing Lagrangian variation of the pressure and density [ $\nabla \cdot \mathbf{U} = 0$ , see (26)]; its parameters do not depend on the adiabatic index. Adding the condition  $\nabla \cdot \mathbf{U} \equiv \Delta\phi = 0$  to (15), it is easy to show that this mode, which is described by the function  $F(z) = \exp\left(-\sqrt{l(l+1)}z/R\right)$  and has the frequency

$$\omega_0^2 = \frac{g}{R} \sqrt{l(l+1)} \quad (21)$$

$$\approx 10^8 g_{14} \left( \frac{10 \text{ km}}{R} \right) \sqrt{l(l+1)} \text{ s}^{-2},$$

exists for any equation of state. Therefore, the frequency  $\omega_0$  will further be used to make the eigenfrequencies of the oscillations dimensionless.

The frequencies  $\omega$  computed here refer to the coordinate system of the stellar envelope [see (9)] and can easily be transformed to the frequencies  $\tilde{\omega}$  as detected by a distant observer:

$$\tilde{\omega} = \omega \sqrt{1 - R_G/R}.$$

### 3.2. Viscous Damping of the Oscillations

In this section, we consider the damping of oscillations with velocity potentials of the form  $e^{i\omega t} Y_{lm}(\Omega) F(r)$  in a spherically symmetrical star under the action of shear viscosity. We take the space-time metric to be flat. This treatment is applicable to the oscillations studied in Section 3.1, since the flat metric (10), which coincides with the metric for a thin spherical layer in a flat spacetime, can be introduced in the region, where oscillations are localized. As a result, it is sufficient to consider the oscillation damping time in a flat metric and transform this time [in accordance with (9)] into the frame of a distant observer.

We define the oscillation damping time  $\tau$  as

$$\tau = E/|dE/dt|, \quad (22)$$

where

$$E = \int \varepsilon dV = \int \rho \frac{|U|^2}{2} dV \quad (23)$$

is the total energy of the oscillations and

$$\varepsilon = \frac{1}{4} \left( \rho_0 |U|^2 + \frac{c_s^2}{\rho_0} |\delta\rho|^2 \right)$$

is the energy density of the oscillations at a given point averaged over the period (see, for example, [34]). The additional factor of 1/2 in the expression for  $\varepsilon$  is required due to the averaging over the oscillation period. The integration is carried out over the entire volume of the star (in practice, over the region where the oscillations are localized). We neglect the perturbation of the gravitational potential. The last equality in (23) is determined by the equality of the mean kinetic and potential energies in the case of small harmonic oscillations. Note that a number of authors have considered the damping time for the oscillation amplitude rather than the damping time for the oscillation energy (22).

When calculating the energy using (23), the angular integration can be carried out analytically:

$$E = \frac{1}{2} \int_0^R \rho \left[ (F')^2 + \frac{l(l+1)}{r^2} F^2 \right] r^2 dr.$$

The period-averaged rate of viscous dissipation of the energy is (see, for example, [34])

$$\frac{dE}{dt} = -\frac{1}{4} \int \sigma'_{ik} \left( \frac{\partial U_i^*}{\partial x_k} + \frac{\partial U_k^*}{\partial x_i} \right) dV, \quad (24)$$

where the viscous-stress tensor  $\sigma'_{\alpha\beta}$  is given by (1). As in the computation of the oscillation energy  $E$ , the additional factor of 1/2 is required owing to the averaging over the oscillation period. It is easy to see that the rate of dissipation of energy separates into a sum of terms associated with shear and bulk viscosities. We will only consider the dissipation determined by the shear viscosity. The integration over the angular variables in (24) can be carried out analytically (see the Appendix).

### 3.3. Discussion of the Numerical Results

As an example, we choose a ‘‘canonical’’ model for a neutron star with a mass of  $M = 1.4 M_\odot$  and a radius of  $R = 10$  km. For this model,

$$\omega_0 \approx 1.56 \times 10^5 \left( \frac{l(l+1)}{10^4} \right)^{1/4} \text{ s}^{-1},$$

and for a distant observer

$$\tilde{\omega}_0 \approx 0.766 \omega_0 \approx 1.19 \times 10^5 \left( \frac{l(l+1)}{10^4} \right)^{1/4} \text{ s}^{-1}.$$

The thickness of the outer crust of such a star ( $\rho < 4 \times 10^{11}$  g/cm<sup>3</sup> before the neutron drip point) is  $\approx 410$  m.

The eigenfrequencies of the oscillations were found via a series of iterative trials, testing for the coincidence of the mode number with the number of radial nodes.

#### 3.3.1. Eigenfrequencies of the Oscillations

The dependence of the eigenfrequencies of the oscillations specified by (16) with the boundary conditions (17) and (18) on  $l$  is presented in Figs. 5 and 6. As we indicated above, the frequency of the fundamental mode, which does not have any radial nodes, is determined by (21) for all  $l$ .

With decreasing  $l$ , the oscillations penetrate deeper regions of the outer crust, where the equation of state is softened due to the relativistic nature of the electron gas and beta captures. This gives rise to a gradual decrease in the dimensionless eigenfrequencies of the oscillations. As in the model with the polytropic equation of state [see (20)], the distance between the squares of the dimensionless eigenfrequencies for a fixed  $l$  is nearly constant. The weak approach of the frequencies with growth in the number of radial nodes is due to the penetration of the oscillations to

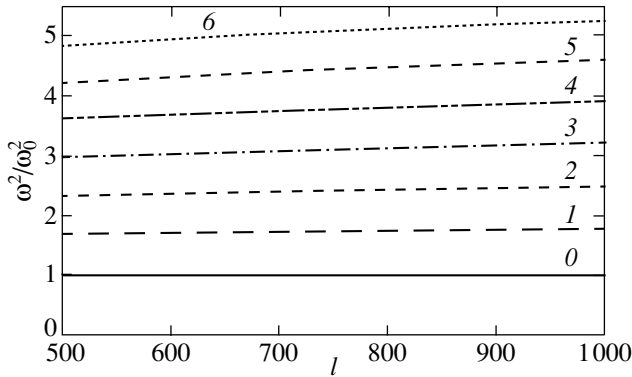


**Fig. 5.** Eigenfrequencies of oscillations localized in the crust of a “canonical” neutron star. The numerical values are normalized to the frequency  $\omega_0$  given by (21). The numbers next to the curves indicate the number of radial nodes.

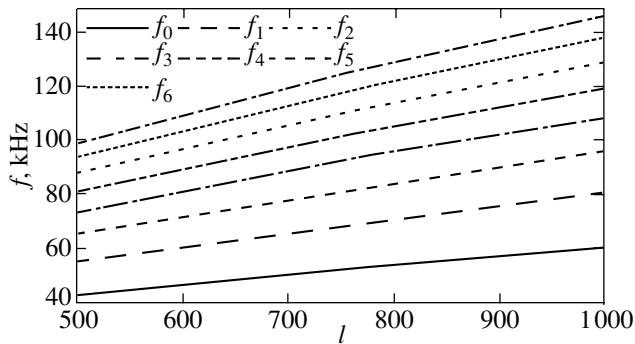


**Fig. 6.** Frequencies of oscillations localized in the crust of a “canonical” neutron star as detected by a distant observer. The subscript of  $f$  denotes the number of radial nodes.

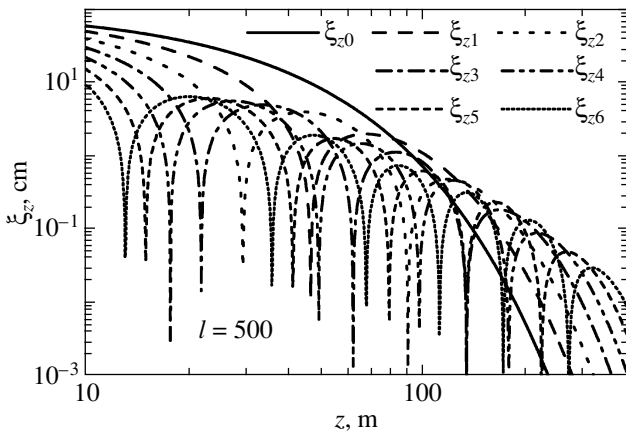


**Fig. 7.** Root-mean-square (in the angular variables) amplitude of the radial displacements of matter for modes with  $l = 500$ . The subscript of  $\xi$  indicates the number of radial nodes. The root-mean-square amplitude of the radial displacements at the stellar surface has been set equal to 1 m.

deeper layers of the star, where the equation of state is softened. When  $l \sim 500$ , the main oscillation energy is localized in the region  $50 \text{ m} \lesssim z \lesssim 400 \text{ m}$ , where the equation of state of the degenerate, relativistic electron gas is described well by the profile of the sound speed. Therefore, the estimate (20) for the eigenfrequencies obtained in the polytropic model for the envelope with polytropic index  $n = 3$  is valid (with accuracy to within several percent).

### 3.3.2. Modes of the Oscillations

Figure 7 presents profiles of the radial displacements of the matter for modes with  $l = 500$ . The mean squared amplitude of the radial displacements of the stellar surface was taken to be 1 m. Since we are considering linear oscillations, this quantity is an arbitrary (sufficiently small) constant that normalizes the solution. It is easy to determine from Fig. 7 the magnitude of the radial displacements in the star for any other amplitude of the radial displacements at the surface. With growth of the depth  $z$ , there is a decrease in the amplitude of the radial displacements  $\xi_z$ , associated with oscillations. At  $z \gtrsim 300 \text{ m}$ , the decrease becomes monotonic and gradually emerges onto the exponential asymptotic (19). This makes it reasonable to speak of the localization of the oscillations in the outer crust of the star.

This effect is manifested even more clearly in the energy density of the oscillations. Figure 8 presents the dependence of the total energy density  $\varepsilon$  averaged over the angular variables as a function of the depth  $z$  for oscillations with  $l = 500$ . The amplitude of the mode is normalized in the same way as in Fig. 7. In our approximation, the energy density of the oscillations is proportional to the square of the normalized amplitude of the radial displacements of the surface. The depicted modes are localized in the outer crust of the neutron star. The energy density of the oscillations varies comparatively weakly within the “critical” depth  $z \lesssim 100\text{--}200 \text{ m}$ , after which it falls off exponentially. The energy density decreases by more than two orders of magnitude toward the boundary between the outer and inner crust of the star.

As was noted in Section 3.3.1, when  $l \sim 500$ , the oscillation frequencies are reproduced well by a polytropic model for the crust. The situation is somewhat different for the eigenmodes. Normalization at the stellar surface is not expedient for these modes, since this model poorly reproduces the structure of the star at low depths  $z \lesssim 40 \text{ m}$ . Consequently, such normalization leads to large errors at the depths of interest to us,  $z \lesssim 100\text{--}200 \text{ m}$ , where the main oscillation energy is concentrated. Therefore, we need some kind of special normalization to compare modes. Figure 9

(like Fig. 8) depicts the angle-averaged energy density of the oscillations  $\varepsilon$  as a function of  $z$ . The symbols show the results of the numerical computations, while the curves show profiles in the polytropic model, normalized so as to bring the results into agreement in the region, where oscillations are localized. We can see that the polytropic model for the outer crust satisfactorily reproduces the energy density of the oscillations at depths of  $60 \text{ m} \lesssim z \lesssim 500 \text{ m}$  for modes with  $l \sim 500$ .

### 3.3.3. Damping of the Oscillations

In the further computations, the neutron-star crust was taken to be isothermal. This approximation describes well the intrinsic temperature profile: the temperature is nearly independent of depth due to the high thermal conductivity of the degenerate electron gas. In our computations, the frequency and damping time of the oscillations did not depend on the normalization amplitude (the amplitude of the radial displacements of the surface).

Figures 10, 11, and 12 present the dependence of the damping time  $\tau$  of the oscillations (for a distant observer) on  $l$  for canonical neutron star with crust temperatures of  $T = 10^7, 10^8, \text{ and } 10^9 \text{ K}$ .

The strong temperature dependence of the oscillation damping time is due to the appreciable decrease in the viscosity with increasing temperature (Fig. 4).

The oscillation damping time can be estimated based on the characteristic parameters of the oscillations:

$$\tau \sim \varepsilon / \dot{\varepsilon} \sim \rho U^2 / \eta \left( \frac{U}{\lambda} \right)^2 \sim \lambda^2 \frac{\rho}{\eta},$$

where  $\dot{\varepsilon}$  is the local viscous-dissipation rate and  $U$  and  $\lambda$  are the characteristic velocity and scale for variations of this quantity in the region of localization of the oscillations.

Let us consider Fig. 11 in more detail. Oscillations with  $l \sim 500$  are localized at  $z \lesssim 100 \text{ m}$  (Fig. 8), which corresponds to densities  $\rho \lesssim 10^{10} \text{ g/cm}^3$ . Under these conditions, the ratio  $\rho/\eta$  is  $\sim 3 \text{ s/cm}^2$  (Fig. 4) and grows with increasing  $l$  (due to the decrease of the density in the region of localization of the oscillations). We present further estimates for modes with  $l \sim 500$ . The scale for variations in the velocity can be estimated as  $\lambda \sim R/l$ . Note that this scale decreases for high modes (with a large number of radial nodes), accelerating the damping of the oscillations. For the fundamental mode (without any radial nodes), the damping time (transformed to the frame of a distant observer) can be estimated as

$$\tau \sim 1.2 \times 10^4 (500/l)^2 \text{ s} \approx 120 (500/l)^2 \text{ day},$$

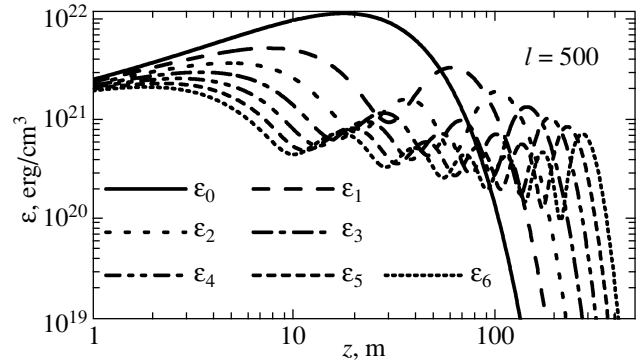


**Fig. 8.** Angle-averaged total energy density of the oscillations  $\varepsilon$  for modes with  $l = 500$ . The subscript of  $\varepsilon$  indicates the number of radial nodes. The mean squared amplitude of the radial displacements at the stellar surface has been set equal to 1 m.

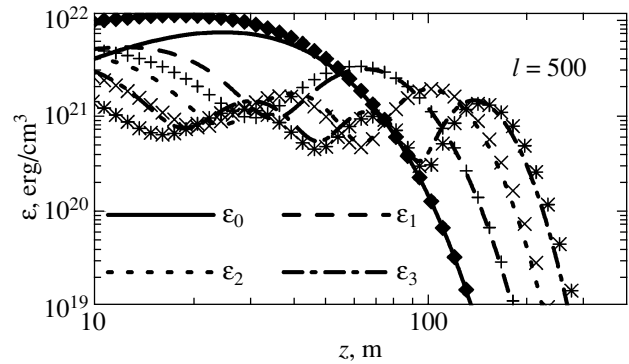


**Fig. 9.** Angle-averaged total energy density of the oscillations  $\varepsilon$  for modes with  $l = 500$ . The subscript indicates the number of radial nodes. The curves show the computed values for the polytropic model, and the symbols show the numerical results for the exact equation of state.

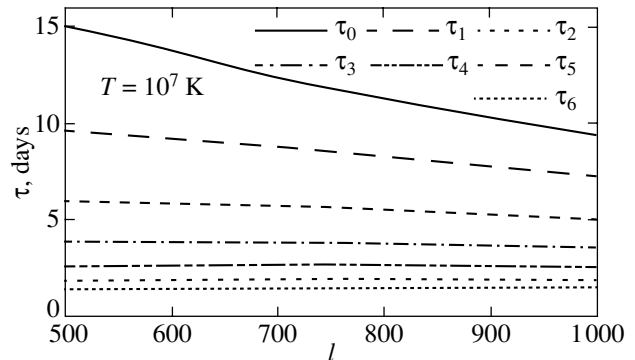


**Fig. 10.** Damping time of the oscillations for a distant observer as a function of  $l$  for a neutron star with a crust temperature of  $T = 10^7 \text{ K}$ . The subscript of  $\tau$  corresponds to the number of radial nodes.

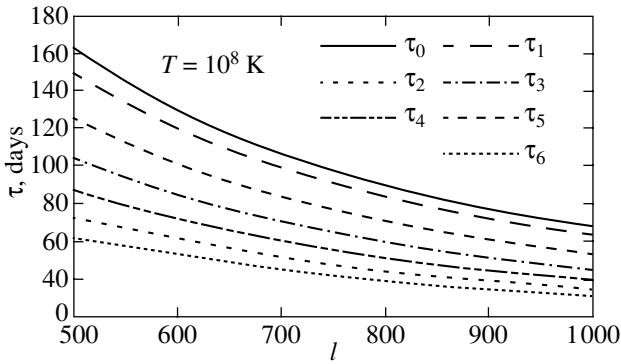


Fig. 11. Same as Fig. 10 but for a crust temperature  $T = 10^8$  K.

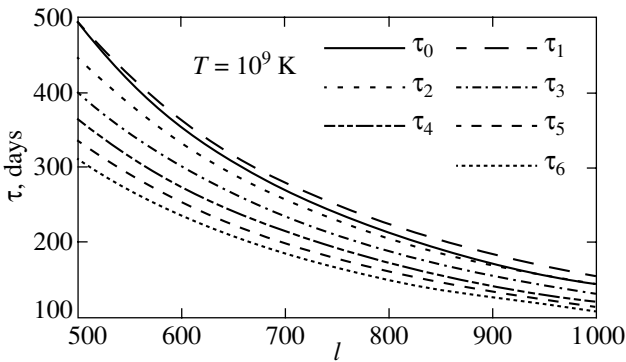


Fig. 12. Same as Fig. 10 but for a crust temperature  $T = 10^9$  K.

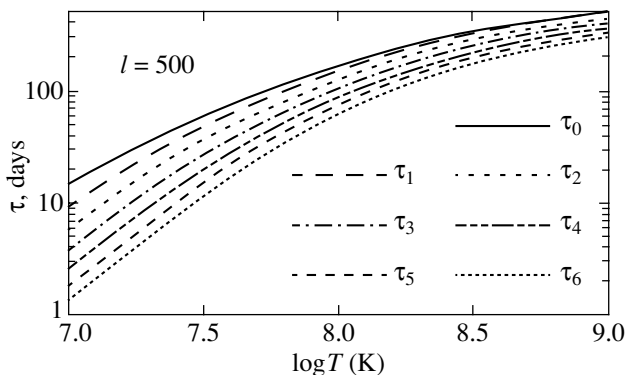


Fig. 13. Damping time of the oscillations as a function of the crust temperature of the neutron star for modes with  $l = 500$ . The subscript indicates the number of radial nodes. The numerical results are presented in the frame of a distant observer.

in good agreement with the numerical results for  $l \sim 500$ . The damping time drop weaker than  $\propto l^{-2}$  is due to the growth in the ratio  $\rho/\eta$  for higher  $l$ , due to the decrease of the density in the region of localization of the oscillations.

For the outer crust of a star with a temperature of  $T = 10^9$  K, the ratio  $\rho/\eta$  does not depend very strongly on the density  $\rho$ . Therefore, the oscillation damping time well obeys the law  $\tau \propto l^{-2}$ .

The dependence of the damping time on the crust temperature is presented in Fig. 13, where we have chosen modes with  $l = 500$  as an example. The damping time grows by approximately two orders of magnitude as the temperature varies from  $10^7$  to  $10^8$  K. When the temperature increases by another order of magnitude, the damping time grows further by a factor of three. This is due to the nonlinear drop in the viscosity with growth in the temperature (Fig. 4).

There exist many other damping mechanisms in addition to the viscous damping of oscillations of a neutron star considered here [14]. For example, damping due to the radiation of gravitational and electromagnetic waves (due to oscillations of the stellar matter with a frozen-in magnetic field) are often studied. In our case, these mechanisms are inefficient due to the high multipolarity considered,  $l \gtrsim 500$ . When  $l$  is high, we expect gravitational or electromagnetic radiation to be generated by an ensemble of closely spaced coherent elementary radiating regions, which radiate in antiphase and cancel each other out. Formally, the weakness of this radiation is manifested by the presence of large factors  $(2l + 1)!!$  in the denominators of the expressions for the radiation intensities (see, for example, [35, 36]). Analysis shows that the damping of the oscillations we consider here is determined to a substantial extent by the shear viscosity.

A detailed analysis of the evolution of the pulse shapes of some radio pulsars provides evidence that high-multipole oscillations are, indeed, excited in them (see, for example, the recent study [37]). However, reliable observational data on the existence of such oscillations have not yet been obtained.

#### 4. CONCLUSIONS

We have carried out computations of the shear viscosity of the dense stellar matter for a broad range of parameters that are typical for the cores of white dwarves and the envelopes of neutron stars. We considered matter consisting of important astrophysical elements from H to Fe at densities from  $10^2$ – $10^4$  g/cm<sup>3</sup> to  $10^7$ – $10^{10}$  g/cm<sup>3</sup>. At higher densities,  $10^{10}$ – $10^{14}$  g/cm<sup>3</sup>, we considered matter with an equilibrium nuclear composition taking into account

the finite size of the atomic nuclei and the distribution of proton charge within the nuclei. Under the conditions described above, the viscosity is determined by the Coulomb scattering of the degenerate electrons by atomic nuclei. We used the modified ion structure factor proposed by Baiko *et al.* [22] and applied by Potekhin *et al.* [1] to compute the thermal and electrical conductivities. In an ionic fluid, this modification approximately takes into account the quasi-ordering in ions positions, which reduces the scattering of electrons by the ions. In the crystalline phase, the new structure factor takes into account multiphonon processes, which are important near the melting temperature  $T_m$ . The new results near the melting point differ appreciably from those of Flowers and Itoh [2, 3] obtained for a Coulomb fluid. The numerical results were approximated by an analytical expression that is convenient for astrophysical applications.

We investigated the frequencies and modes of oscillations localized in the outer crust of a neutron star in a plane-parallel approximation. A polytropic model for the crust can reproduce the eigenfrequencies of the oscillation modes with multipolarity  $l \sim 500$  reasonably well. The viscous-damping time for the oscillations was also computed. There is a sharp decrease in the damping time with increasing temperature of the neutron-star crust. For example, for a neutron star with mass  $M = 1.4 M_\odot$ , radius  $R = 10$  km, and a crust temperature of  $T = 10^8$  K, the damping time for the fundamental mode with  $l = 500$  is  $\sim 160$  day. When the temperature decreases to  $T \sim 10^7$  K, the damping time falls to  $\sim 15$  day.

In our computations, we used a model of the ground state matter for the neutron star crust with a smoothed dependence of the parameters of the atomic nuclei on the density of the matter. More accurate computations would require the use of an exact model for the equilibrium nuclear composition, in which this composition was varied with depth in the crust in a jumpwise fashion (there arises a series of weak phase transitions of the first kind at specific depths). The presence of these jumps could strengthen the damping of the oscillations. We plan on considering this problem in a future study.

#### ACKNOWLEDGMENTS

The authors thank D. Gough for reprints of his papers related to oscillations of polytropic stellar envelopes, and W. Dziembowski, who pointed out these works to us. We are also grateful to K.P. Levenfish and A.Yu. Potekhin for useful discussions. This work was supported by a student grant of the Non-Profit Foundation “Dynasty” and the International Center for Fundamental Physics in Moscow, the Russian Foundation for Basic Research (RFFI-IAU grant

no. 03-02-06803 and project no. 05-02-16245), and the Program of Support for Leading Scientific Schools of Russia (NSh-1115.2003.2).

#### APPENDIX

##### INTEGRATION OF THE LOCAL RATE OF VISCOUS DISSIPATION OF ENERGY OVER THE ANGULAR VARIABLES

When calculating the angular integral in (24), it is convenient to introduce the notation

$$\tilde{\sigma}_{ik} \equiv \frac{\partial U_i}{\partial x_k} + \frac{\partial U_k}{\partial x_i}.$$

Then, the part of (24) that is associated with the shear viscosity can be written as

$$\begin{aligned} \frac{dE}{dt} &= -\frac{1}{4} \int_0^R \eta r^2 dr \int \left[ \tilde{\sigma}_{ik} \tilde{\sigma}_{ki}^* - \frac{4}{3} |\nabla \mathbf{U}|^2 \right] d\Omega \\ &= -\frac{1}{4} \int_0^R r^2 \eta \left( I_1 - \frac{4}{3} I_2 \right) dr, \end{aligned} \quad (25)$$

where  $d\Omega$  is an element of solid angle,

$$I_1 \equiv \int \tilde{\sigma}_{ik} \tilde{\sigma}_{ki}^* d\Omega \quad \text{and} \quad I_2 \equiv \int |\nabla \mathbf{U}|^2 d\Omega.$$

Here, we have assumed that the unperturbed star is spherically symmetrical, so that the shear viscosity  $\eta$  does not depend on the angular variables. The integrals  $I_1$  and  $I_2$  were computed analytically for velocities of the form  $\mathbf{U} = \nabla \phi$ , where the velocity potential is  $\phi = e^{i\omega t} Y_{lm}(\theta, \varphi) F(r)$ .

The integral  $I_1$  can be computed if we write the components of the tensor  $\tilde{\sigma}_{ik}$  in spherical coordinates (see, for example, [34]). After this, the integration over the angles can be carried out analytically (using the properties of the function  $Y_{lm}(\theta, \varphi)$ ; see, for example, [32]). This yields

$$\begin{aligned} I_1 &= 4 \left\{ (F'')^2 + 2 \frac{1+l(l+1)}{r^2} (F')^2 \right. \\ &\quad \left. - 6 \frac{l(l+1)}{r^3} F' F + l(l+1) \frac{1+l(l+1)}{r^4} F^2 \right\} \\ &\approx 4 \left\{ (F'')^2 + 2 \frac{l(l+1)}{R^2} (F')^2 \right. \\ &\quad \left. + l(l+1) \frac{l(l+1)}{R^4} F^2 \right\}, \end{aligned}$$

where the last equality is valid in the plane-parallel layer approximation.

Let us now consider the integral  $I_2$ . For this, we write the divergence of the velocity:

$$\begin{aligned} \nabla \mathbf{U} = \Delta \phi &= \left( \frac{1}{r^2} \frac{\partial}{\partial r} r^2 \frac{\partial F}{\partial r} Y_{lm}(\theta, \varphi) \right. \\ &\quad \left. + F \Delta_{\Omega} Y_{lm}(\theta, \varphi) \right) e^{i\omega t} \\ &= \left( F'' + \frac{2F'}{r} - \frac{l(l+1)}{r^2} F \right) Y_{lm}(\theta, \varphi) e^{i\omega t}, \end{aligned} \quad (26)$$

where  $\Delta_{\Omega}$  is the angular part of the Laplacian. The integral  $I_2$  can easily be calculated:

$$\begin{aligned} I_2 &= \left( F'' + \frac{2F'}{r} - \frac{l(l+1)}{r^2} F \right)^2 \\ &\approx \left( F'' - \frac{l(l+1)}{R^2} F \right)^2, \end{aligned}$$

where this last equality is valid in the plane-parallel layer approximation. As expected, expression (25) does not depend on the azimuthal number  $m$  (due to the spherical symmetry of the unperturbed star). It can be shown that it is nonnegative for all allowed values  $l = 0, 1, 2, \dots$

## REFERENCES

1. A. Y. Potekhin, D. A. Baiko, P. Hansel, and D. G. Yakovlev, *Astron. Astrophys.* **346**, 345 (1999).
2. E. Flowers and N. Itoh, *Astrophys. J.* **206**, 218 (1976).
3. E. Flowers and N. Itoh, *Astrophys. J.* **230**, 847 (1979).
4. R. Nandkumar and C. J. Pethick, *Mon. Not. R. Astron. Soc.* **209**, 511 (1984).
5. N. Itoh, Y. Kohyama, N. Matsumoto, and M. Seki, *Astrophys. J.* **285**, 758 (1984).
6. N. Itoh, H. Hayashi, and Y. Kohyama, *Astrophys. J.* **418**, 405 (1993).
7. K. S. Thorne and A. Campolattaro, *Astrophys. J.* **149**, 591 (1967).
8. R. Price and K. S. Thorne, *Astrophys. J.* **155**, 163 (1969).
9. K. S. Thorne, *Astrophys. J.* **158**, 1 (1969).
10. K. S. Thorne, *Astrophys. J.* **158**, 997 (1969).
11. A. Campolattaro and K. S. Thorne, *Astrophys. J.* **159**, 847 (1970).
12. J. R. Ipser and K. S. Thorne, *Astrophys. J.* **181**, 181 (1973).
13. P. N. McDermott, H. M. Van Horn, and J. F. Scholl, *Astrophys. J.* **268**, 837 (1983).
14. P. N. McDermott, H. M. Van Horn, and C. J. Hansen, *Astrophys. J.* **325**, 725 (1988).
15. N. Stergioulas, *Living Rev. Relativ.* **6**, 3 (2003).
16. V. M. Kaspi, *Young Neutron Stars and Their Environments*, Ed. by F. Camilo and B. M. Gaensler (Astron. Soc. Pac., San Francisco, 2004), p. 231.
17. H. DeWitt, W. Slattery, D. Baiko, and D. Yakovlev, *Contrib. Plasma Phys.* **41**, 251 (2001).
18. L. D. Landau and E. M. Lifshitz, *Theory of Elasticity* (Nauka, Moscow, 1968; Pergamon Press, Oxford, 1986).
19. J. M. Ziman, *Electrons and Phonons* (Clarendon, Oxford, 1960; Inostrannaya Literatura, Moscow, 1962).
20. D. A. Baiko and D. G. Yakovlev, *Pis'ma Astron. Zh.* **21**, 784 (1995) [*Astron. Lett.* **21**, 702 (1995)].
21. V. B. Berestetskii, E. M. Lifshitz, and L. P. Pitaevskii, *Quantum Electrodynamics* (Fizmatlit, Moscow, 2001; Pergamon Press, Oxford, 1982).
22. D. A. Baiko, A. D. Kaminker, A. Y. Potekhin, and D. G. Yakovlev, *Phys. Rev. Lett.* **81**, 5556 (1998).
23. D. G. Yakovlev, *Astron. Zh.* **64**, 661 (1987) [*Sov. Astron.* **31**, 347 (1987)].
24. A. Y. Potekhin, G. Chabrier, and D. G. Yakovlev, *Astron. Astrophys.* **323**, 415 (1997).
25. B. Jancovici, *Nuovo Cimento* **25**, 428 (1962).
26. A. D. Kaminker, C. J. Pethick, A. Y. Potekhin, *et al.*, *Astron. Astrophys.* **343**, 1009 (1999).
27. O. Y. Gnedin, D. G. Yakovlev, and A. Y. Potekhin, *Mon. Not. R. Astron. Soc.* **324**, 725 (2001).
28. M. Abramowitz and I. A. Stegun, *Handbook of Mathematical Functions*, Ed. by M. Abramowitz and I. A. Stegun (Dover, New York, 1971; Nauka, Moscow, 1979).
29. M. Prakash, T. L. Ainsworth, and J. M. Lattimer, *Phys. Rev. Lett.* **61**, 2518 (1988).
30. S. L. Shapiro and S. A. Teukolsky, *Black Holes, White Dwarves, and Neutron Stars: the Physics of Compact Objects* (Wiley, New York, 1983; Mir, Moscow, 1985), Vols. 1, 2.
31. H. Lamb, *Proc. R. Soc. A* **84**, 551 (1911).
32. D. A. Varshalovich, A. N. Moskalev, and V. K. Khersonskii, *Quantum Theory of Angular Momentum* (Nauka, Leningrad, 1975; World Sci., Singapore, 1988).
33. D. O. Gough, *Astrophysical Fluid Dynamics*, Ed. by J.-P. Zahn and J. Zinn-Justin (Elsevier, Amsterdam, 1993), p. 399.
34. L. D. Landau and E. M. Lifshitz, *Fluid Mechanics* (Fizmatgiz, Moscow, 2001; Pergamon Press, Oxford, 1987).
35. E. Balbinski and B. F. Schutz, *Mon. Not. R. Astron. Soc.* **200**, 43 (1982).
36. P. N. McDermott, M. P. Savedoff, H. M. Van Horn, *et al.*, *Astrophys. J.* **281**, 746 (1984).
37. J. Clemens and R. Rosen, *Astrophys. J.* **609**, 340 (2004).

*Translated by D. Gabuzda*